Accepted Manuscript

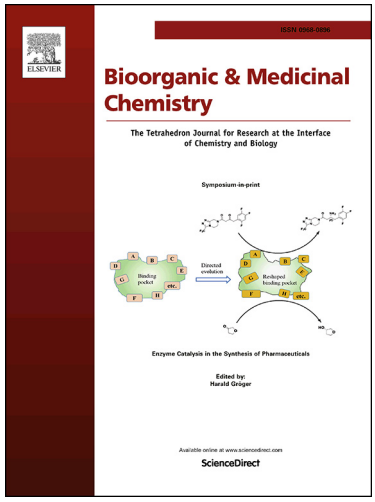

Microwave-assisted organic synthesis, structure–activity relationship, kinetics and molecular docking studies of non-cytotoxic benzamide derivatives as selective butyrylcholinesterase inhibitors

Sheeba Wajid, Asma Khatoon, Maria Aqeel Khan, Humaira Zafar, Shama Kanwal, Atta-ur-Rahman, M. Iqbal Choudhary, Fatima Z. Basha

PII: S0968-0896(19)30927-7
DOI: https://doi.org/10.1016/j.bmc.2019.07.015
Reference: BMC 14999

To appear in: *Bioorganic & Medicinal Chemistry*

Received Date: 3 June 2019
Revised Date: 5 July 2019
Accepted Date: 9 July 2019

Please cite this article as: Wajid, S., Khatoon, A., Khan, M.A., Zafar, H., Kanwal, S., Atta-ur-Rahman, Iqbal Choudhary, M., Basha, F.Z., Microwave-assisted organic synthesis, structure–activity relationship, kinetics and molecular docking studies of non-cytotoxic benzamide derivatives as selective butyrylcholinesterase inhibitors, *Bioorganic & Medicinal Chemistry* (2019), doi: https://doi.org/10.1016/j.bmc.2019.07.015

Microwave-assisted organic synthesis, structure–activity relationship, kinetics and molecular docking studies of non-cytotoxic benzamide derivatives as selective butyrylcholinesterase inhibitors

Sheeba Wajid[a], Asma Khatoon[a], Maria Aqeel Khan[a], Humaira Zafar[b], Shama Kanwal[a], Atta-ur-Rahman[a], M. Iqbal Choudhary[a,b*], and Fatima Z. Basha[a*]

[a]*H. E. J. Research Institute of Chemistry, International Center for Chemical and Biology Science, University of Karachi-75270, Pakistan.*

[b]*Dr. Panjwani Center for Molecular Medicine and Drug Research (PCMD), International Center for Chemical and Biological Sciences, University of Karachi, Karachi, Pakistan*

E-mail: bashafz@gmail.com

iqbal.chaudhary@iccbs.com

Abstract

A series of benzamide derivatives **1-12** with various functional groups (-H, -Br, -F, $-OCH_3$, $-OC_2H_5$, and $-NO_2$) were synthesized using an economic, and facile Microwave-Assisted Organic Synthesis, and evaluated for acetylcholinesterase (ACHE) and butyrylcholinesterase (BCHE) activity *in vitro*. Structure–activity relationship showed that the substitution of -Br group influenced the inhibitory activity against BCHE enzyme. Synthesized compounds were found to be selective inhibitors of BCHE. In addition, all compounds **1-12** were found to be non-cytotoxic, as compared with standard cycloheximide (IC_{50} = 0.8 ± 0.2 μM). Among them, compound **3** revealed the most potent BCHE inhibitory activity (IC_{50} = 0.8 ± 0.6 μM) when compared with standard galantamine hydrobromide (IC_{50} = 40.83 ± 0.37 μM). Enzyme kinetic studies indicated that compounds **1**, **3-4**, and **7-8** showed mixed mode of inhibition against BCHE, while compounds **2**, **5-6** and **9** exhibited an uncompetitive pattern of inhibition. Molecular docking studies further highlighted the interaction of these inhibitors with catalytically important amino acid residues, such as Glu197, Hip438, Phe329 and many others.

***Keywords*:**

Benzamides, Green Chemistry, Microwave-Assisted Organic Synthesis, Acetylcholinesterase, Butyrylcholinesterase, Enzyme Inhibition, Alzheimer disease.

1. Introduction

Alzheimer's disease (AD) is a neurological disorder of senior population. This disease was identified by Dr. Alois Alzheimer in 1906 who also discovered plaques and tangles in the AD brain [1, 2]. AD may arise with the destruction of nerve cells that also affects the function of brain. Due to neurodegeneration lifespan of the patients declines that make AD among top ten causes of death in developed countries [3, 4]. Globally 35 million population has been affected from AD [5] and it is hypothesized that by the end of 2050, 1 person in 85 people will be affected. Cholinesterases, comprises of acetylcholinesterse (ACHE) [EC 3.1.1.7], and butyrylcholinesterase (BCHE) [EC 3.1.1.8], are renowned serine hydrolases, and have nucleophilic serine residue in the active sites [6]. Acetylcholinesterase (ACHE) is found in erythrocytes, nerve endings, lungs, spleen and in the all compartments of brain. Butyrylcholinesterase (BCHE) has capability to hydrolyse various choline-based esters. BCHE is precisely found in peripheral tissues, brain, serum, neurons, and glial cells [7-9]. BCHE have ability to hydrolyze many drugs, like cocaine, acetylcholine, and succinylcholine [10-12], and thus play a vital role in neurodegenerative disorder. In the last stages of Alzheimer`s disease, there is an increase in the development of amyloid plaque and neurofibrillary tangles with the increase expression of BCHE enzyme [13]. Researchers also found that level of acetylcholinesterase (ACHE) is reduced when incubated with Aβ fibrils, while BCHE remains active [14]. This study highlights the significance of developing selective BCHE inhibitors for the treatment of AD.

Recently, several natural products or their derivatives were discovered as potential therapy for the treatment of AD. Galantamine, donepezil, and rivastigmine are well known cholinesterase inhibitors that have proven to enhance cognitive function with mild to moderate AD patients [15]. Selective BCHE inhibitors elevate brain acetylcholine, improve cognition and decline β-amyloid, and thus may serve as modern therapy in the treatment of AD. Therefore, there is a need to identify BCHE inhibitors. In current study, we focused to study a series of benzamide derivatives for BCHE enzyme inhibition *in vitro*.

Benzamide derivatives have been reported for a variety of pharmacological activities, such as acetylcholinesterase [16], antimicrobial, antioxidant [17], chymotrypsin [18], antiasthmatic [19], anti-leukotriene [20] and anti-HIV [21] activities, *etc*. Currently, a number of potent drugs are available that possess amide functionality as a key structural element, such as aripiprazole (antipsychotic), phenacetin (analgesic and antipyretic) and atorvastatin (lipid-lowering drug) [22-24]. Beside other biological properties, this class is also identified as potent cholinesterase inhibitors. Gao and co-workers have reported benzamide and policnamide analogues as selective ACHE inhibitors [16]. Darvesh *et al.* have reported alkyl and aryl derivatives of phenothiazine as selective BCHE inhibitors [25, 26]. We have designed a series of benzamide derivatives, and studied their effect on activity and selectivity (BCHE: ACHE) by varying properties of molecule, such as hydrolytic properties *via* adding two chloro groups at *N*-aryl part, and changing substituents at acyl part, of benzamide moiety (Fig. 1).

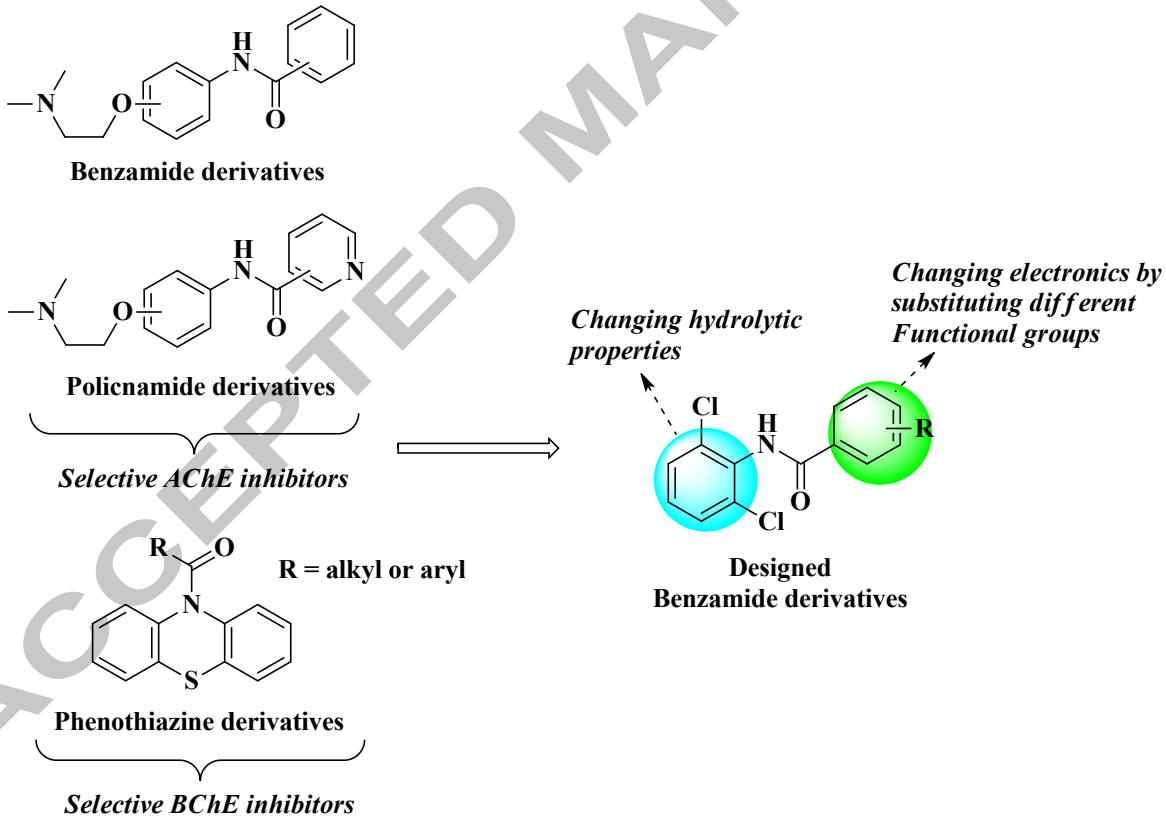

Fig. 1. Designing of benzamide analogues.

Various methods have been reported on amide synthesis, but base-catalyzed reaction of amines or anilines with benzoyl chlorides is the common reported strategy. Most of the amidation

reactions make use of hazardous solvents [dichloromethane (DCM), toluene, and tetrahydrofuran (THF)] and toxic bases (sodium hydride, and tertiary amines), which add disadvantages to the method and decreased its utility [27]. Green synthetic methodologies are considered as safe alternates to the traditional strategies. Their environmentally benign conditions and efficiency increased the utility of these methods. Microwave-Assisted Organic Synthesis (MAOS) is one of the considerable green routes by Gedbye and Giguere/Majetich in 1986 [28]. Short reaction time, simpler and easier workups, high yield, environmentally benign, highly efficient, selective, and clean reactions are important attributes of this protocol [29-31]. This method has been emerged as an effective synthetic strategy for many transformations, such as etherification, esterification, hydrolysis, rearrangement, and addition reactions, *etc.* [32-37]. It is also an efficient method in peptide synthesis, material sciences, biochemical processes, polymer chemistry, and nanotechnology [38-46]. Based on the efficiency of this method, a series of benzamide derivatives of 2,6-dichloroaniline was prepared using solvent-free and base-free MAOS methodology with the goal of identifying potential BCHE inhibitors. For this, the inhibition potential of newly synthesized compounds against ACHE and BCHE enzymes, their Structure-Activity Relationship, enzyme kinetic parameters and molecular docking studies was investigated.

2. Experimental

2.1. Material and methods

All chemicals were of analytical grade. Butrylcholinesterase (BCHE) (equine serum) (Sigma Aldrich), Acetylcholinesterase (ACHE) (electric eel) (Sigma Aldrich), 5,5`-Dithio*bis*(2-nitrobenzoic acid) (DTNB) (D218200) (Sigma Aldrich), butrylthiocholine chloride (1866-16-6), acetylthiocholine iodide (6050-81-3) and sodium dihydrogen phosphate (NaH_2PO_4) (543840) were bought from Sigma Aldrich. Galantamine hydrobromide (65789) was isolated from commercially available tablets, donepezil (Sigma Aldrich), and 2,6-dichloroaniline (820430) were obtained from Merck, Acros organics, Alfa Aesar, and Sigma Aldrich, respectively. At 300 MHz and 400 MHz, and using appropriate deuterated solvents, NMR spectra were recorded on spectrometer (Bruker). EI- and ESI-Mass spectra were recorded on a Finningan MAT-321A (Germany). Infrared (IR) spectra were obtained on Bruker vector 22 spectrometer (United States).

2.2. Synthesis of benzamide derivatives 1-12

General Procedure: 0.5 mmol of benzoyl chlorides and 1.0 mmol of 2,6-dichloroaniline was flushed with nitrogen gas in microwave (MW) vial. At 130 °C and 200 W, reaction was irradiated under microwave for 15 mins. The mixture was washed with bicarbonate solution and 5% EtOAc: *n*-hexanes to obtain benzamide derivatives **1-12**.

*2.2.1. N-(2,6-Dichlorophenyl) benzamide (**1**)* [47]

Yield: 95%; white solid; IR υ cm^{-1} (KBr disk): 3239, 1655 (amide), 1570, 1515; ^{1}H-NMR: (400 MHz, DMSO-d_6): δ 10.26 (s, 1H, N*H*), 8.00 (d, 2H, $J_{2',3'/6',5'}$ = 7.6 Hz, H-2', H-6'), 7.52-7.64 (m, 5H, H-3, H-5, H-3', H-5', H-4'), 7.40 (t, 1H, $J_{4,(3,5)}$ = 8.0 Hz, H-4); ESI MS: *m/z* : 269 $[M+H+4]^+$, 267 $[M+H+2]^+$, 265 $[M+H]^+$.

*2.2.2. 2-Bromo-N-(2,6-dichlorophenyl)benzamide (**2**)* CAS # 10282-64-1

Yield: 80%; white solid; IR υ cm^{-1} (KBr disk): 3184, 1671 (amide), 1575, 1514; ^{1}H-NMR: (400 MHz, DMSO-d_6): δ 10.42 (s, 1H, N*H*), 7.74 (d, 1H, $J_{2',3'}$ = 8.0 Hz, H-5'), 7.57-7.61 (m, 3H, H-3, H-5, H-3'), 7.52 (t, 1H, $J_{4',(3',5')}$ = 6.8 Hz, H-4'), 7.44 (dd, 1H, $J_{5',4'}$ = 7.6 Hz, $J_{5',2'}$ = 1.6 Hz, H-5'), 7.40 (t, 1H, $J_{4,(3,5)}$ = 8.4 Hz, H-4); ESI MS: *m/z* : 348 $[M+H+4]^+$, 346 $[M+H+2]^+$, 344 $[M+H]^+$.

*2.2.3. 4-Bromo-N-(2,6-dichlorophenyl)benzamide (**3**)* CAS # 282091-65-0

Yield: 95%; white solid; IR υ cm^{-1} (KBr disk): 3221, 1651 (amide), 1578, 1511; ^{1}H-NMR: (300 MHz, DMSO-d_6): δ 10.36 (s, 1H, N*H*), 7.92 (d, 2H, $J_{2',3'/6',5'}$ = 8.4 Hz, H-2', H-6'), 7.75 (d, 2H, $J_{3',2'/5',6'}$ = 8.4 Hz, H-3', H-5'), 7.58 (d, 2H, $J_{3,4/5,4}$ = 8.4 Hz, H-3, H-5), 7.37 (t, 1H, $J_{4,(3,5)}$ = 8.1 Hz, H-4); ESI MS: *m/z*: 348 $[M+H+4]^+$, 346 $[M+H+2]^+$, 344 $[M+H]^+$.

*2.2.4. N-(2,6-Dichlorophenyl)-4-fluorobenzamide (**4**)* CAS # 330196-46-8

Yield: 69%; white solid; IR υ cm^{-1} (KBr disk): 3225, 1658 (amide), 1615, 1529; ^{1}H-NMR: (300 MHz, DMSO-d_6): δ 10.29 (s, 1H, N*H*), 8.04 (dd, 2H, $J_{2',3'/6',5'}$ = 8.7 Hz, $J_{2',6'/6',3'}$ = 5.7 Hz, H-2', H-6'), 7.57 (d, 2H, $J_{3,4/5,4}$ = 8.4 Hz, H-3, H-5), 7.32-7.39 (m, 3H, H-4, H-3', H-5'); ESI MS: *m/z*: 288 $[M+H+4]^+$, 286 $[M+H+2]^+$, 284 $[M+H]^+$.

*2.2.5. N-(2,6-Dichlorophenyl)-2,4-difluorobenzamide (**5**)* CAS # 948649-43-2

Yield: 63%; white solid; IR υ cm^{-1} (KBr disk): 3225, 1658, 1615 (amide), 1529; ^{1}H-NMR: (400 MHz, DMSO-d_6): δ 10.27 (s, 1H, N*H*), 7.77-7.83 (m, 1H, H-6'), 7.60 (d, 2H, $J_{3,4/5,4}$ = 8.4 Hz, H-3, H-5), 7.38-7.46 (m, 2H, H-3', H-4), 7.25 (td, 1H, $J_{5',(4',6')}$ = 8.4 Hz, $J_{5',(3',6')}$ = 1.6 Hz, H-5'); ESI MS: *m/z*: 306 $[M+H+4]^+$, 304 $[M+H+2]^+$, 302 $[M+H]^+$.

*2.2.6. N-(2,6-Dichlorophenyl)-2,6-difluorobenzamide (**6**)* CAS # 937635-92-2

Yield: 90%; white solid; IR υ cm^{-1} (KBr disk): 3196, 1662 (amide), 1627, 1526; ^{1}H-NMR: (400 MHz, DMSO-d_6): δ 10.69 (s, 1H, N*H*), 7.55-7.63 (m, 3H, H-3, H-5, H-4'), 7.41 (t, 1H, $J_{4,(3,5)}$ = 8.0 Hz, H-4), (t, 2H, $J_{3',(2',4')/5',(4',6')}$ = 8.0 Hz, H-3', H-5');ESI MS: *m/z*: 306 $[M+H+4]^+$, 304 $[M+H+2]^+$, 302 $[M+H]^+$.

*2.2.7. N-(2,6-Dichlorophenyl)-3-methoxybenzamide (**7**)* CAS # 199726-36-8

Yield: 72%; white solid; IR υ cm^{-1} (KBr disk): 3203, 1647 (amide), 1594, 1512; ^{1}H-NMR: (400 MHz, DMSO-d_6): δ 10.26 (s, 1H, N*H*), 7.60 (d, 3H, $J_{3,4/5,4/4',5'}$ = 8.0 Hz, H-3, H-5, H-4'), 7.53 (s, 1H, H-2'), 7.45 (t, 1H, $J_{5',(6',4')}$ = 8.0 Hz, H-5'), 7.40 (t, 1H, $J_{4,(3,5)}$ = 8.4 Hz, H-4), 7.18 (dd, 1H, $J_{6',5'}$ = 8.0 Hz, $J_{6',2'}$ = 2.0 Hz, H-6'), 3.83 (s, 3H, OCH_3-3'); ESI MS: *m/z*: 300 $[M+H+4]^+$, 298 $[M+H+2]^+$, 296 $[M+H]^+$.

*2.2.8. N-(2,6-Dichlorophenyl)-4-methoxybenzamide (**8**)* CAS # 157491-16-2

Yield: 75%; white solid; IR υ cm^{-1} (KBr disk): 3251, 1650 (amide), 1560; ^{1}H-NMR: (400 MHz, DMSO-d_6): δ 10.10 (s, 1H, N*H*), 7.99 (d, 2H, $J_{3',2'/5',6'}$ = 8.4 Hz, H-3', H-5'), 7.58 (d, 2H, $J_{3,4/5,4}$ = 8.0 Hz, H-3, H-5), 7.38 (t, 1H, $J_{4,(3,5)}$ = 8.4 Hz, H-4), 7.08 (d, 2H, $J_{2',3'/6',5'}$ = 8.8 Hz, H-2', H-6'), 3.85 (s, 3H, OCH_3-4'); ESI MS: *m/z*: 300 $[M+H+4]^+$, 298 $[M+H+2]^+$, 296 $[M+H]^+$.

*2.2.9. N-(2,6-Dichlorophenyl)-3,4,5-trimethoxybenzamide (**9**)* CAS # 198009-97-1

Yield: 74%; white solid; IR υ cm^{-1} (KBr disk): 3287, 1670 (amide), 1588, 1490; ^{1}H-NMR: (400 MHz, DMSO-d_6): δ 10.20 (s, 1H, N*H*), 7.60 (d, 2H, $J_{3,4/5,4}$ = 8.4 Hz, H-3, H-5), 7.42 (t, 1H, $J_{4,(3,5)}$= 8.4 Hz, H-4), 7.35 (s, 2H, H-1', H-6'), 3.85 (s, 6H, OCH_3-3', OCH_3-5'), 3.73 (s, 3H, OCH_3-4');; EI MS *m/z* (% rel. abund.): 355 (M^++2, 16), 355 (M^+, 24), 195 (100).

*2.2.10. N-(2,6-Dichlorophenyl)-2-ethoxybenzamide (**10**)* CAS # 314055-43-1

Yield: 57%; white solid; IR υ cm^{-1} (KBr disk): 3298, 1655 (amide), 1600, 1503; ^{1}H-NMR: (400 MHz, DMSO-d_6): δ 9.86 (s, 1H, N*H*), 7.78 (dd, 1H, $J_{5',4'}$ = 7.6 Hz, $J_{5',2'}$ = 1.6 Hz, H-5'), 7.56 (d, 2H, $J_{3,4/5,4}$ = 8.4 Hz, H-3, H-5), 7.52 (t, 1H, $J_{4',(3',5')}$ = 8.0 Hz, H-4'), 7.37 (t, 1H, $J_{4,(3,5)}$ = 8.0 Hz, H-4), 7.21 (d, 1H, $J_{2',3'}$ = 8.0 Hz, H-2'), 7.07 (t, 1H, $J_{3',(5',4')}$ = 8.0 Hz, H-3'), 4.21-4.26 (m, 2H, CH_2-6'), 1.41 (t, 3H, CH_3-6'); ESI MS: *m/z*: 314 $[M+H+4]^+$, 312 $[M+H+2]^+$, 310 $[M+H]^+$.

*2.2.11. N-(2,6-Dichlorophenyl)-3-nitrobenzamide (**11**)* CAS # 351155-08-3

Yield: 83%; white solid; IR υ cm^{-1} (KBr disk): 3225, 1652 (amide), 1571, 1524; ^{1}H-NMR: (300 MHz, DMSO-d_6): δ 10.71 (s, 1H, N*H*), 8.79 (s, 1H, H-2), 8.43-8.47 (m, 1H, H-4'), 8.42 (d, 1H, $J_{6',5'}$ = 7.8 Hz, H-6'), 7.84 (t, 1H, $J_{5',(4',6')}$ = 8.1 Hz, H-5'), 7.60 (d, 2H, $J_{3,4/5,4}$ = 8.1 Hz, H-3, H-5), 7.39 (t, 1H, $J_{4,(3,5)}$ = 7.9 Hz, H-4); ESI MS: *m/z*: 315 $[M+H+4]^+$, 313 $[M+H+2]^+$, 311 $[M+H]^+$.

*2.2.12. N-(2,6-Dichlorophenyl)-4-methyl-3-nitrobenzamide (**12**)* CAS # 351492-12-1

Yield: 98%; white solid; IR υ cm^{-1} (KBr disk): 3229, 1652 (amide), 1570, 1519; ^{1}H-NMR: (400 MHz, DMSO-d_6): δ 10.60 (s, 1H, N*H*), 8.60 (s, 1H, H-2'), 8.23 (dd, 1H, $J_{6',5'}$ = 8.0 Hz, $J_{6',2'}$ = 1.2 Hz, H-6'), 7.72 (d, 1H, $J_{5',6'}$ = 8.4 Hz, H-5'), 7.62 (d, 2H, $J_{3,4/5,4}$ = 8.0 Hz, H-3, H-5), 7.42 (t, 1H, $J_{4,(3,5)}$ = 8.4 Hz, H-4), 3.33 (s, 3H, CH_3); ESI MS: *m/z*: 329 $[M+H+4]^+$, 327 $[M+H+2]^+$, 325 $[M+H]^+$.

2.3. BCHE inhibition assay

To determine the mean inhibitory concentrations (IC_{50}), and kinetic mechanisms of the effective compounds, Ellman's assay was performed with slight modifications [48]. All reactions were performed in 96-well microplates, and the reaction volume was kept as 200 μL. BCHE enzyme (51.732 mU/, 20 μL) was incubated individually with test compounds (0.5 mM) (dissolved in methanol) in 150 μL of 100 mM sodium phosphate buffer (pH 8.0), and incubated for 15 minutes at 25 °C. The reaction was initiated by adding 10 μL of pre-prepared butyrylthiocholine chloride (0.5 mM) substrate and in the dark for 15 minutes, and DTNB (0.5 mM), which is a chemical reagent used to identify thiol groups in the sample was added and plate was read at 412nm in spectrophotometer.

2.4. ACHE inhibition assay

ACHE Inhibitory activity was performed with slight modification of Ellman's assay [48]. All reactions were performed in 96-well microplates, and the reaction volume was kept as 200 μL. ACHE enzyme (0.002 mU/, 20 μL) was incubated individually with test compounds (0.5 mM) (dissolved in methanol) in 150 μL of 100 mM sodium phosphate buffer (pH 8.0), and incubated for 15 minutes at 25 °C. The reaction was initiated by adding 10 μL of pre-prepared acetylthiocholine iodide (0.5 mM) substrate and DTNB in the dark for 15 minutes, and plate was read at 412 nm in spectrophotometer.

2.5. Cytotoxicity assay

MTT (3-[4,5-dimethylthiazole-2-yl]-2,5-diphenyltetrazolium bromide) colorimetric assay was used to perform cytotoxicity of all compounds in 96 well flat-bottomed micro plates. Assay was initiated with the addition of 100 μL of media with $3x10^5$ cells. All the cells got attached to the surface of plate. Media was removed after 24 hours with the addition of fresh media (180 μL) and 20 μL of test compound (1 to 30 μM). The plate was placed under carbon dioxide incubator (5%) with 90% humidity at 37 °C for 48 hours. After incubation, MTT dye (200 μL) was added. The plates were then incubated for 4 hours. Living cells form formazan crystals which were dissolved by adding 100 μL of DMSO [49]. Absorbance was measured at 540 nm. EZ-Fit software was used to calculate IC_{50} values.

2.6. Molecular docking studies

To understand the receptor-ligand interactions of selected butrylcholinesterase inhibitors, molecular docking studies were performed using Maestro Schrödinger2018-1. Crystal structure human butyrylcholinesterase in complex with the substrate analog butyrylthiocholine (1P0P) was used for the docking studies. Protein Preparation Wizard using OPLS3 force field was employed to prepare the receptor and in order to add missing hydrogens. *Ligprep* module was used to prepare the ligands in correct protonation and ionization states [50, 51].

Since most of the inhibitors showed mixed type inhibition, they were docked in active site of butyrylcholinesterase. For the few uncompetitive inhibitors, sitemap was used to generate possible allosteric sites. Among them, the top ranked site was used for the docking of these

ligands. The receptor grid in both the allosteric and active sites has dimensions of 15Å x 15Å x 15Å, and ligands were docked using extra precision mode [52, 53].

3. Result and discussion

3.1. Chemistry

Different substituted benzamides **1-12** were synthesized by reacting acid chlorides with 2,6-dichloroaniline (Scheme-1).

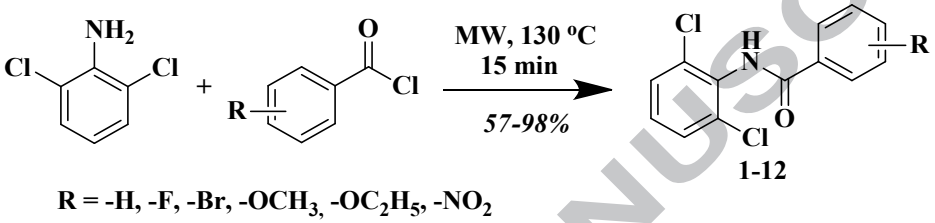

Scheme-1. Synthesis of benzamide derivatives **1-12**.

For optimization, several conditions were used, as shown in Table-1. Initially, reaction was done using different solvents, such as DCM and THF, with triethylamine (NEt_3) as a base. Results revealed that reaction was completed after overnight stirring and desired benzamide was obtained in 20-21% yields, with anhydride formation as a major side product (entry 1-2). Refluxing reaction to 50 °C using NEt_3 as base and THF as solvent, decreased reaction time, however, no appreciable change in amount of desired product was obtained (entry 3). Poor yields and use of hazardous solvents, switched our attention towards solvent-free reaction protocol. For this, varying temperatures (80 °C, 100 °C and 130 °C) were used to explore best solvent-free condition in the presence of NEt_3 as a base. No appreciable change in % yield was observed; however, time of reaction is reduced with increase in temperature (entry 4-6). Switching to solvent-free as well as base-free conditions slightly vary time and amount of product (entry 7). In above given conditions, one equivalent of acid halide and 2 equivalents of aniline were used. Reversing equivalences of two reacting partners and heating at 130 °C in solvent-free and base (NEt_3)-free conditions didn't show any appreciable change. Besides, anhydride was obtained in all conditions, which was very difficult to remove from product. Due to less yield, unwanted side product formation and purification *via* column chromatography, MW-assisted solvent-free and

base-free conditions were explored for the synthesis of benzamide. Interestingly, these conditions provide benzamide product in 75% yield within 0.25 h (15 mins) at 130 °C (entry 8). No anhydride formation as side product was observed and precipitates of product (benzamide) were easily separated by filtration. For additional insights into scope of this protocol, a series of benzamide derivatives **1-12** was prepared in 57-98% yields (Table-2). All the compounds were previously reported [47], but present study is the first report of benzamides (**1-12**) using MW-assisted organic synthesis.

Table-1: Optimization of benzamide derivative 1.

ENTRY	BASE	SOLVENT	TEMPERATURE (°C)	TIME (h)	% YIELD (%)
1	NEt_3	DCM	room temperature	16	21
2	NEt_3	THF	room temperature	16	20
3	NEt_3	THF	50	5	24
4	NEt_3	-	80	4	15
5	NEt_3	-	100	3	17
6	NEt_3	-	130	1.5	20
7	-	-	130	2	15
8	-	-	130/MW	0.25	75

3.2. Structure-activity relationship

Benzamide derivatives **1-12**, substituted with different functional groups (-H, -Br, -F, $-OCH_3$, $-OC_2H_5$, and $-NO_2$) at various positions, were evaluated for their BCHE inhibitory activity

(Table-2). Our parent compound **1** (IC_{50} = 1.3 ± 0.9 μM) was found to be tenfold potent than the standard donepezil (IC_{50} = 8.4 ± 0.34 μM). Therefore, we studied the effect of various electron donating and accepting substitutions on benzamide moiety. Among the halogen derivatives (**2-6**), it was observed that -Br at *ortho* and *para* position of compound **2** (IC_{50} = 1.1 ± 1.7 μM) and **3** (IC_{50} = 0.8 ± 0.6 μM), respectively, showed excellent BCHE inhibitory activity. However, activity was decreased when -Br group at *para* position (compound **3**) was replaced with -F group in compound **4** (IC_{50} = 16.1 ± 1.2 μM). The substitution of additional *ortho* -F group at *para* position in compound **5** (IC_{50} = 18.7 ± 1.2 μM), showed a slight decrease in activity, as compared to compound **4**. In contrast, activity was further reduced while switching two -F groups to two *ortho* positions in compound **6** (IC_{50} = 12.6 ± 0.2 μM). Comparison of methoxy substitution at *meta* position in compound **7** (IC_{50} = 5.5 ± 0.5 μM) exhibited good activity than the standard donepezil (IC_{50} = 8.4 ± 0.34 μM). However, methoxy substitution at *para* position of compound **8** (IC_{50} = 11.3 ± 1.6 μM) and *tri*methoxy substitution in compound **9** (IC_{50} = 20.8 ± 0.6 μM) showed slight decline in the activity as compared to compound **7**. In contrast, the ethoxy substitution in compound **10** (IC_{50} = 6.0 ± 0.5 μM) showed significant activity as compared with standard galantamine hydrobromide (IC_{50} = 40.83 ± 0.37 μM). A marked decline in activity occurred due to the presence of methoxy and -NO_2 groups at *para* and *meta* positions, respectively, of compound **12** (IC_{50} = 165.0 ± 2.0 μM). However, activity was completely lost due to the presence of a -NO_2 at *para* position in compound **11**.

Benzamide derivatives were also evaluated for their ACHE inhibitory activity. None of the compounds showed inhibitory activity against ACHE enzyme. Therefore, synthesized compounds displayed selective inhibition against BCHE enzyme.

Table-2: ChE inhibitory activities of benzamide derivatives 1-12.

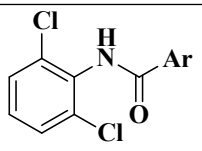

COMPOUND	Ar	% INHIBITION	IC_{50} (μM) ± S.E.M.		% YIELD
			BCHE	ACHE	

1	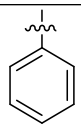	**100.0**	**1.3 ± 0.9***	**inactive**	**75**
2	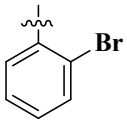	**88.0**	**1.1 ± 1.7***	**inactive**	**80**
3	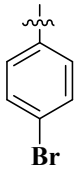	**84.0**	**0.8 ± 0.6***	**inactive**	**95**
4	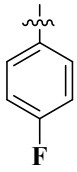	**86.5**	**16.1 ± 1.2**	**inactive**	**69**
5	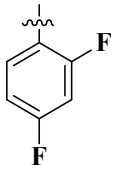	**80.7**	**18.7 ± 1.2**	**inactive**	**63**
6	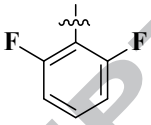	**70.6**	**12.6 ± 0.2**	**inactive**	**90**
7	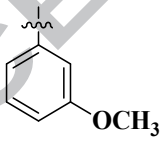	**95.2**	**5.5 ± 0.5***	**inactive**	**72**
8	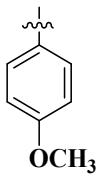	**90.7**	**11.3 ± 1.6**	**inactive**	**75**

9	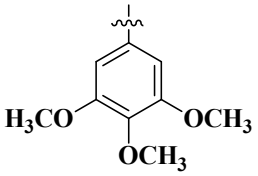	**69.16**	**20.8 ± 0.6**	**inactive**	**74**
10	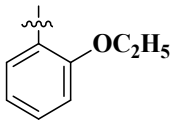	**112.2**	**6.0 ± 0.5***	**inactive**	**57**
11	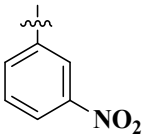	**-**	**inactive**	**inactive**	**83**
12	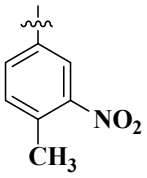	**69.1**	**165 ± 2.0**	**inactive**	**98**
Donepezil			**8.4 ± 0.37**	**2.8 ± 0.7**	
Galantamine hydrochloride			**40.83 ± 0.37**	**3.25 ± 0.3**	

* More potent as compared to standard (Donepezil): IC_{50} = 8.4 ± 0.37 μM.

3.3. Cytotoxicity

Cytotoxicity evaluation of benzamide derivatives **1-12** against 3T3 cell lines and cycloheximide as standard, showed them as non-cytotoxic compounds (Fig. 2).

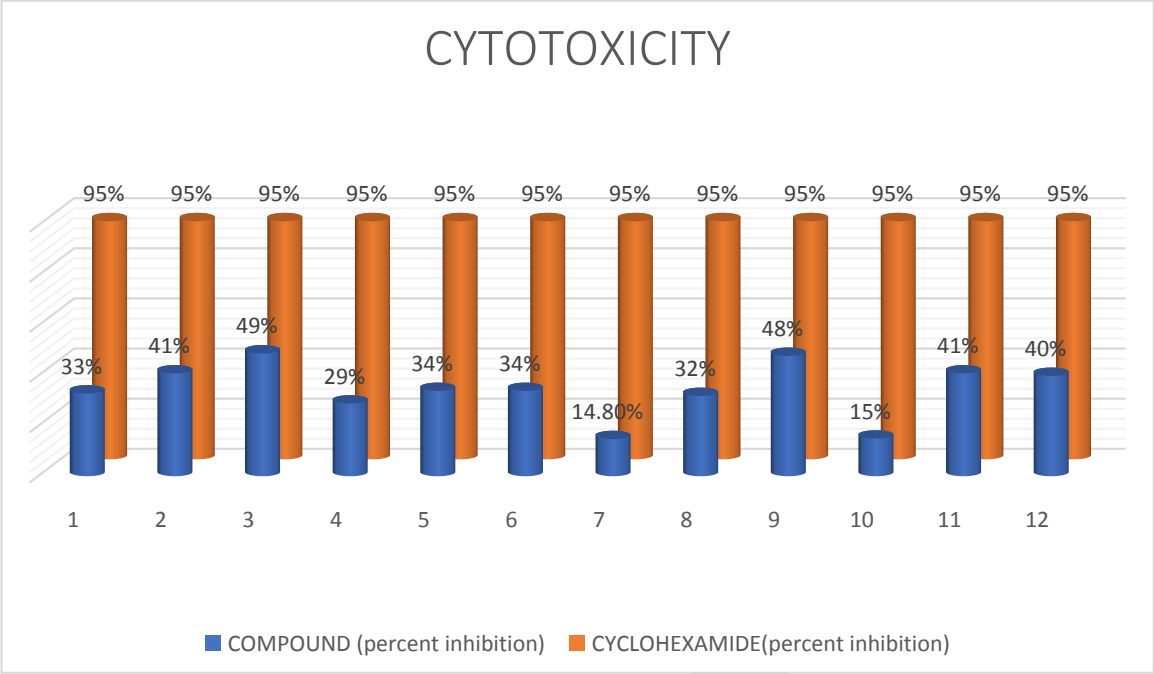

Standard (Cycloheximide) = IC_{50} = 0.8 ± 0.2 µM

Fig. 2. Cytotoxicity evaluation of benzamide derivatives **1-12**.

3.4. Kinetic parameters of inhibition by benzamide derivatives

Kinetics studies of most active compounds were performed to study the mechanism of inhibition (Table-3). Inhibitor's effect was studied by plotting reciprocal of the reaction rate against the reciprocal of substrate concentrations as Lineweaver-Burk plot. Secondary replots of Lineweaver-Burk plot (slope *vs* concentration of inhibitor) and Dixon plots (1/*Vmax vs* inhibitor concentration) were used to confirm the modes of inhibition. Various kinetic parameters were analyzed such as *Km* (substrate concentration at which enzyme velocity is half of the maximum), and *Vmax* (maximum velocity of the enzyme). Compounds **7** and **9** are shown below as representative examples (**Fig. 3** and **4**). Compound **1**, **3-4**, and **7-8** showed a mixed-type of inhibition, as apparent *Km* increased while apparent *Vmax* decreased. This mode is obtained when inhibitor can bind to the active site as well as to enzyme-substrate complex. On contrary, compounds **2**, **5**, **6**, and **9** showed uncompetitive inhibitor as their apparent *Vmax* and *Km* decreased.

Table-3: Kinetic studies of benzamide derivatives.

Compound	IC_{50} (Mean ± S.E.M μM)	*Ki* (μM)	Type of Inhibition
1	1.3 ± 0.9*	4.4 ± 0.3	Mixed
2	1.1 ± 1.7*	2.4 ± 0.8	Uncompetitive
3	0.8 ± 0.6*	2.6 ± 0.7	Mixed
4	16.1 ± 1.2*	9.9 ± 0.1	Mixed
5	18.7 ± 1.2*	27.6 ± 0.4	Uncompetitive
6	12.6 ± 0.2*	5.6 ± 0.8	Uncompetitive
7	5.5 ± 0.5*	13.0 ± 0.2	Mixed
8	11.3 ± 1.6*	18.0 ± 0.4	Mixed
9	20.8 ± 0.6*	23.5 ± 0.2	Uncompetitive
Galantamine hydrochloride (Standard)	**40.83 ± 0.37**	**21.5 ± 0.7**	**Mixed**

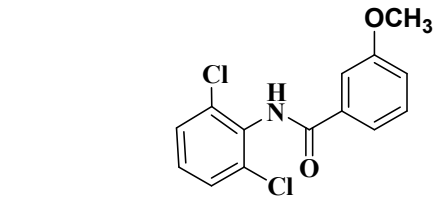

***N*-(2,6-Dichlorophenyl)-3-methoxybenzamide (7)**

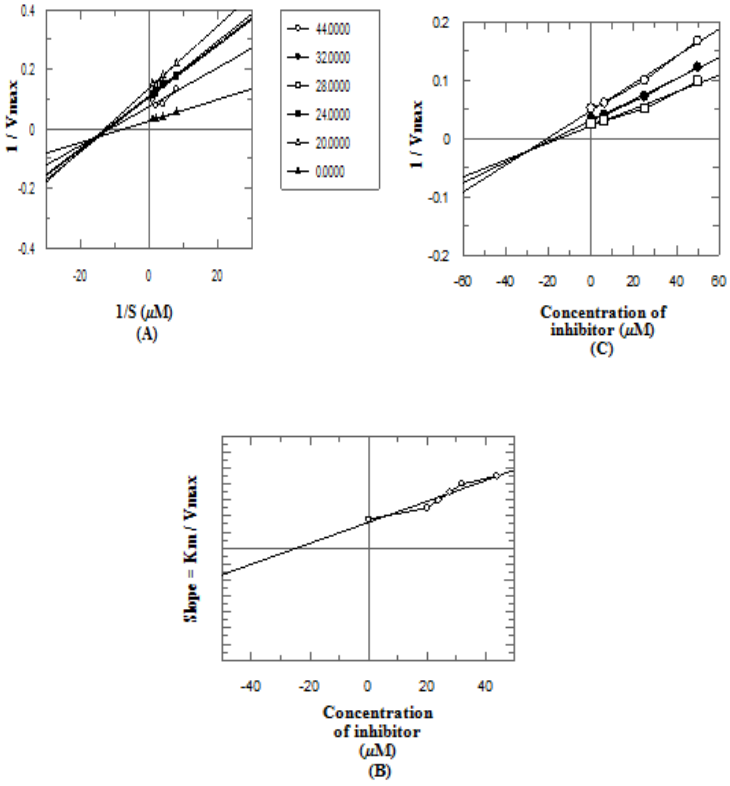

Figure-3: Graphical representation of kinetic parameters and inhibition of butrylcholinesterase activity by compound **7**.
Graph (A) shows Line-weaver-Burk plot, Inhibitor concentrations = 36, 32, 28, and 24 μM.
▼= control
Graph (B) shows secondary replot of Lineweaver-Burk plot
Graph (C) shows Dixon plot

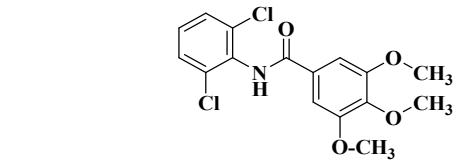

N-(2,6-Dichlorophenyl)-3,4,5-trimethoxybenzamide (9)

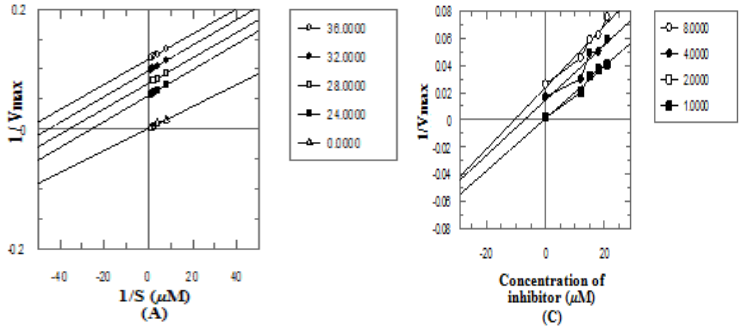

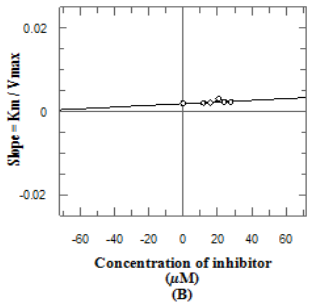

Figure-4: Graphical representation of kinetic parameters and inhibition of butrylcholinesterase activity by compound **9**.
Graph (A) shows Line-weaver-Burk plot, Inhibitor concentrations = 36, 32, 28, and 24 μM.
▼= control
Graph (B) shows secondary replot of Lineweaver-Burk plot
Graph (C) shows Dixon plot

3.5. Molecular docking studies of benzamide derivatives

Molecular docking studies were carried out to understand the interaction of active ligands with the amino acid residues of butrylcholinesterase. Crystal structure of human butyrylcholinesterase in complex with the substrate analog butrylthiocholine (1P0P) was used. The structure of BCHE is well characterized using X-ray studies. It consists of an acyl pocket (Val288, and Leu286), a catalytic triad (Glu325, Ser198, and Hip438), an oxyanion hole (Gly116, Gly117, and Ala199), an anion site (Trp82, Tyr128, and Phe329), and a peripheral anionic site (Asp70, and Tyr332) (Fig. 5) [54].

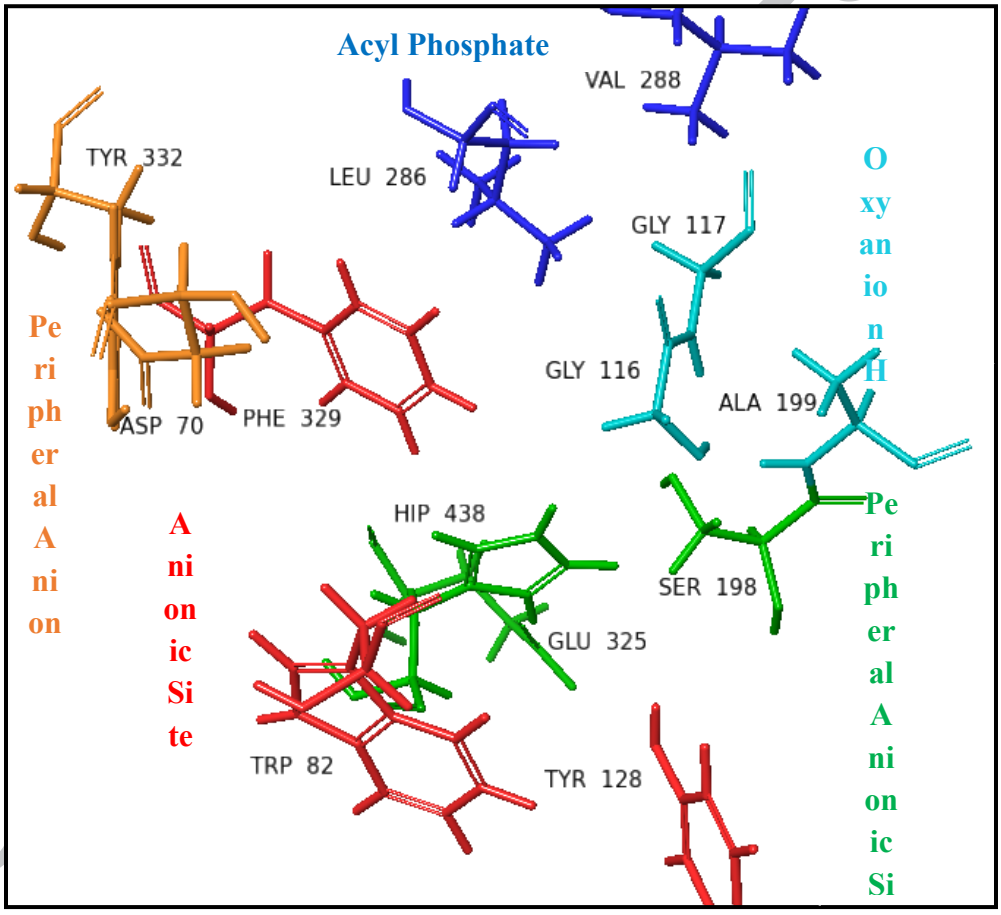

Fig. 5. Active site of human butrylcholinesterase (1P0P) indicating the catalytically important amino acid residues.

The standard inhibitor galantamine hydrobromide was docked into the active site of the enzyme. The standard inhibitor was able to form hydrogen bonds with Hip438 and Asp70. Both the interacting amino acid residues are catalytically important as Hip438 is part of the catalytic triad, while Asp70 belongs to the peripheral anionic site.

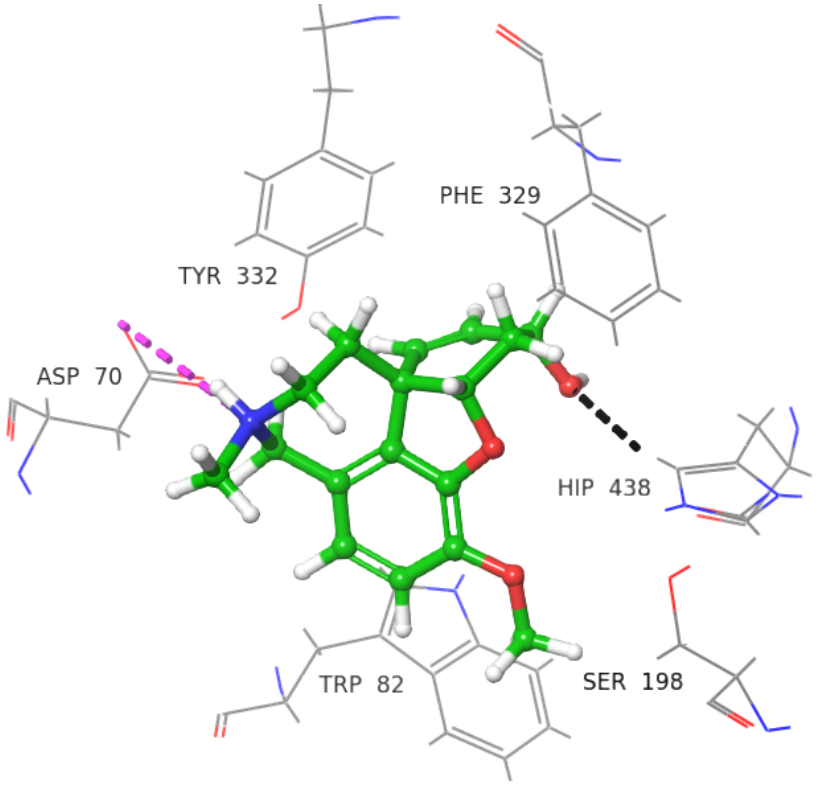

Fig. 6. 3D Representation of docked pose of galantamine hydrobromide (IC_{50} = 40.83 ± 0.8 μM). Two hydrogen bonds are shown with Asp70 and Hip438.

Compounds **1**, **3-4**, and **7-8** were also found to be mixed type inhibitors in our kinetic studies, so they were docked into the active site. The parent compound **1** with no substitution on benzamide moiety showed hydrogen bonding with Glu197 (**Fig. 7**). Compound **3** with Br group at *para* position showed H-bond with Pro285, while the aromatic ring was involved in π-π stacking interactions with Phe329 in the anionic site (Fig. 8). The replacement of Br with flouro group in compound **4** slightly changed the docked pose of this compound and it formed H-bond with HIP438 in the peripheral anionic site (Fig. 9).

Compound **7** with OCH_3 group at *meta* position also showed H-bond with HIP438 in the peripheral anionic site (Fig. 10). Although the change in position of OCH_3 group from *meta* to *para* in compound **8** showed H-bond with Pro285. The π-π stacking interaction was also observed with Phe239 (Fig. 11).

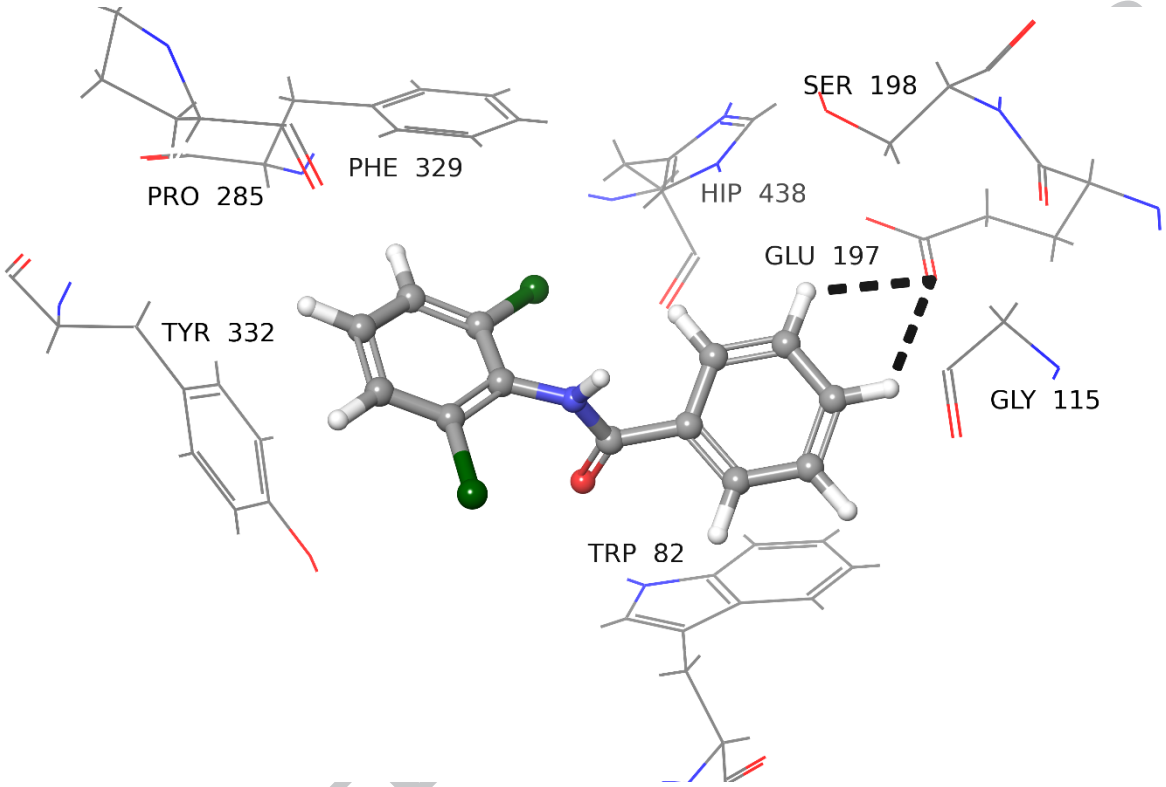

Fig. 7. 3D Representation of docked pose of compound **1** (IC_{50} = 1.3 ± 0.9 μM). Two hydrogen bonds are shown with Glu197.

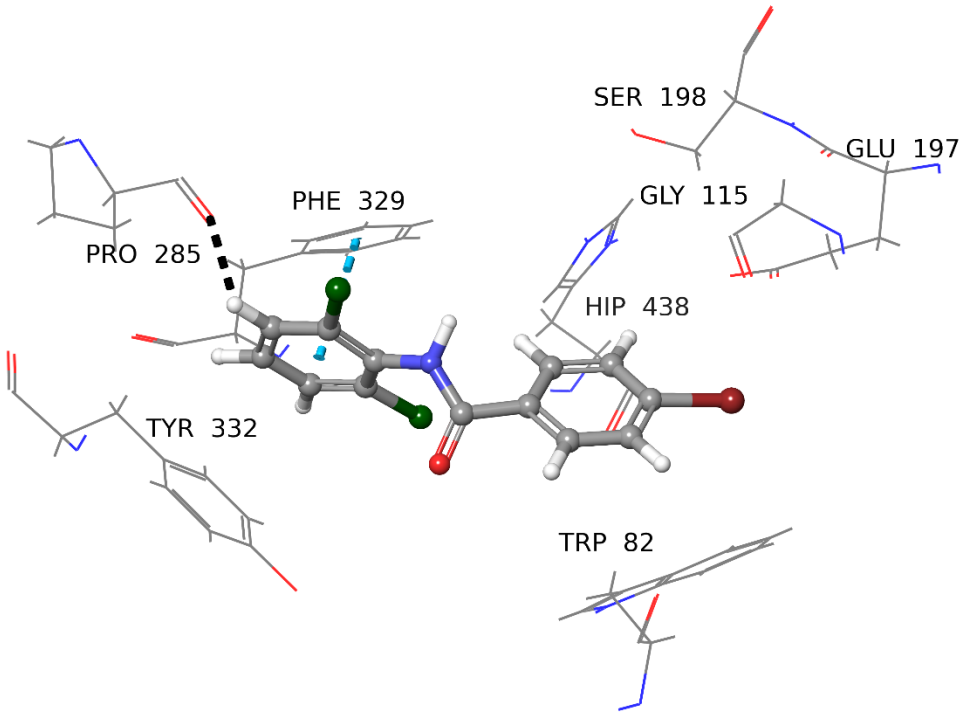

Fig. 8. 3D Representation of docked pose of compound **3** (IC_{50} = 0.8 ± 0.6 μM). A hydrogen bond is shown with Pro285 (black dotted lines) and π-π stacking interaction with Phe329 (blue dotted line).

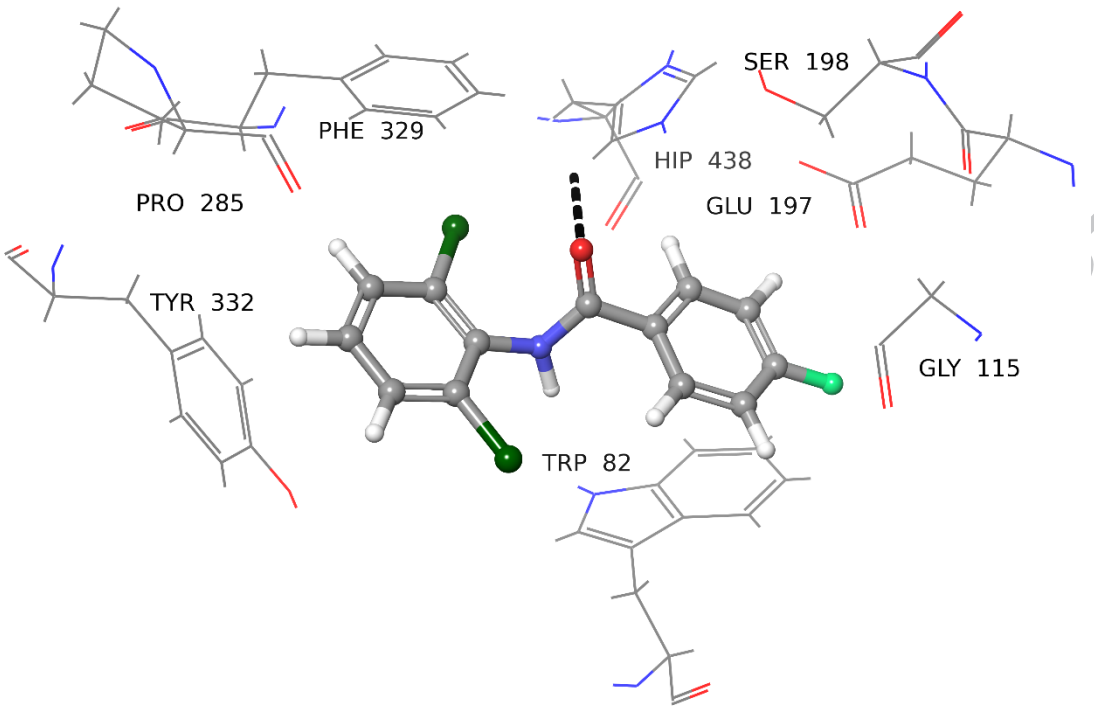

Fig. 9. 3D Representation of docked pose of compound **4** (IC_{50} = 16.1 ± 1.2 μM). A hydrogen bond is shown with Hip438.

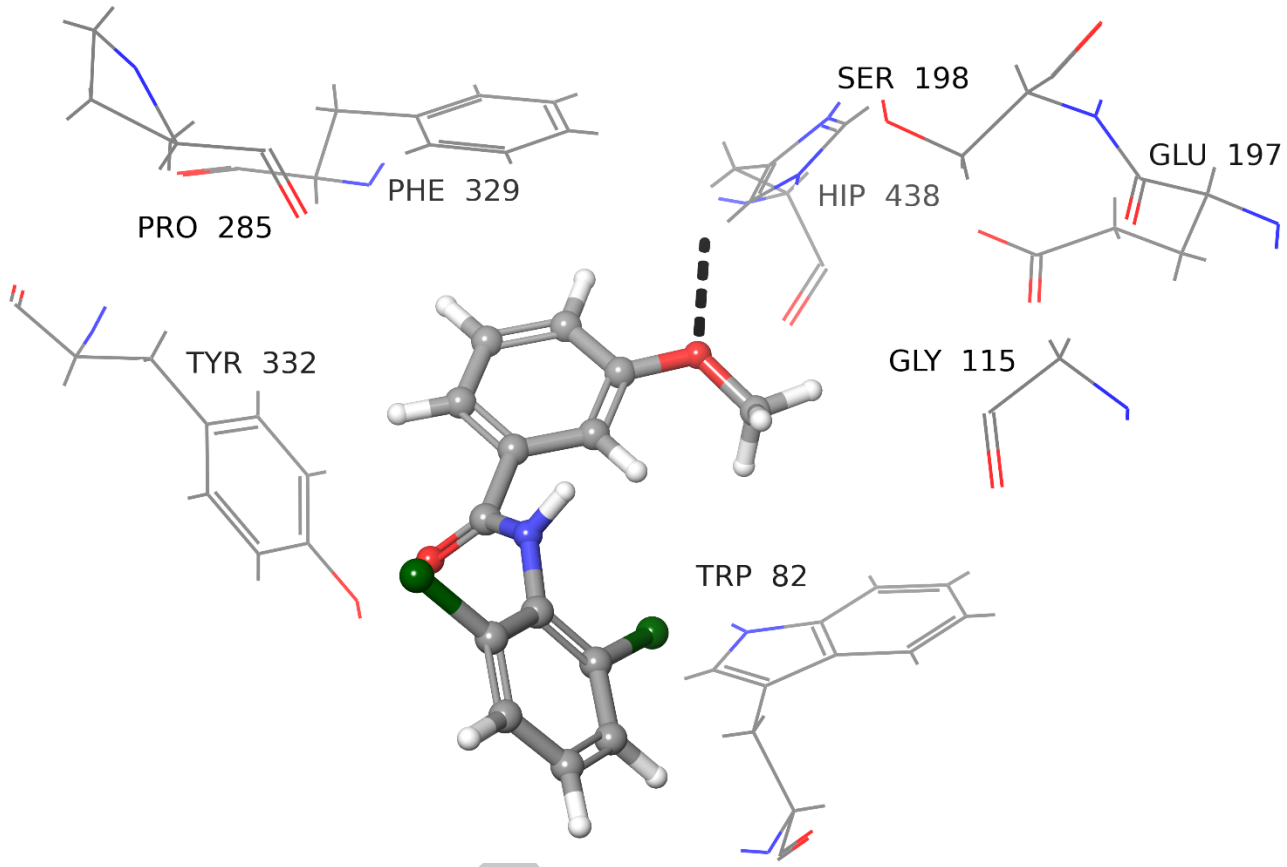

Fig. 10. 3D Representation of docked pose of compound **7** (IC_{50} = 5.5 ± 0.5 μM). Compound **7** interacted with Hip438 *via* H-bonding.

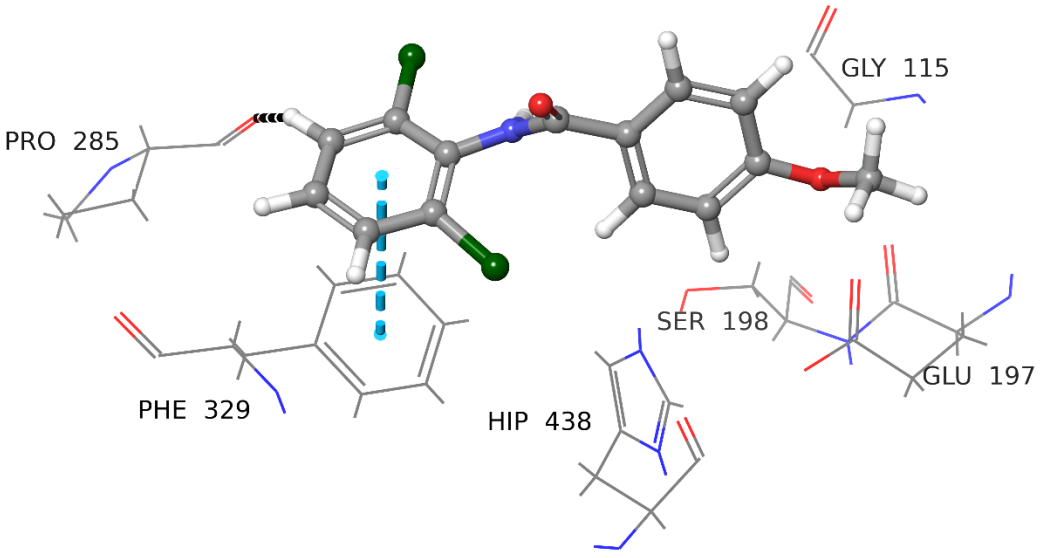

Fig. 11. 3D Representation of docked pose of compound **8** (IC_{50} = 11.3 ± 1.6 μM). Compound **8** interacted with Pro285 and Phe329 *via* H-bonding (black dotted lines) , and π-π stacking interactions (blue dotted lines), respectively.

The uncompetitive inhibitors (**2**, **5**, **6**, and **9**) interacted with the amino acid residues of the allosteric sites (identified *via* sitemap analysis). For instance, compound **2** with Br group at *ortho* position showed H- bonds with Asn228 and Asp304 (Fig. 12). Compound **5** with diflouro substitution at *ortho* and *para* positions showed H-bonds with Asn228 and Thr-523 (Fig. 13).

The difluro substitutions at two *ortho* positions in compound **6**, decreased the three hydrogen bonds (in compound **5**) to only one with Asn228 (Fig. 14). While the H-bond with Thr523 was retained. Compound **9** with tri-methoxy substitutions at *ortho*, *meta*, and *para* positions showed H-bond with Asn228 and Tyr396 (Fig. 15).

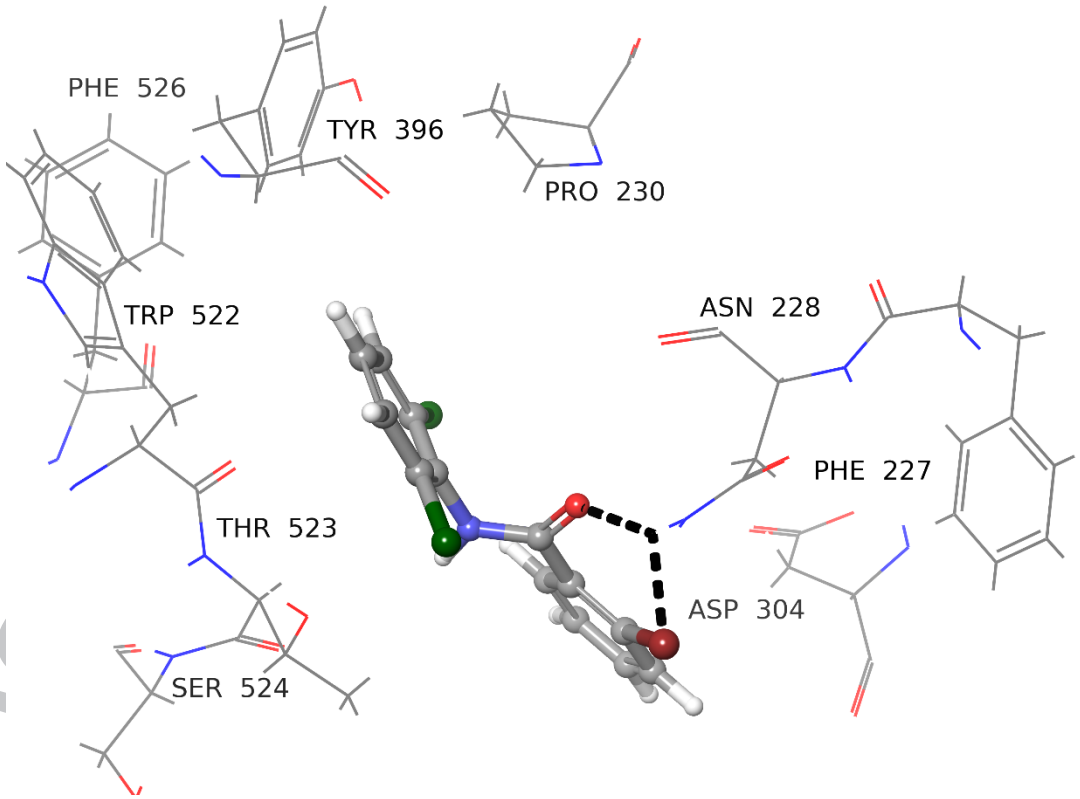

Fig. 12. 3D Representation of docked pose of compound **2** (IC_{50} = 1.1 ± 1.7 μM). The ligand showed H-bonds with Asn228 .

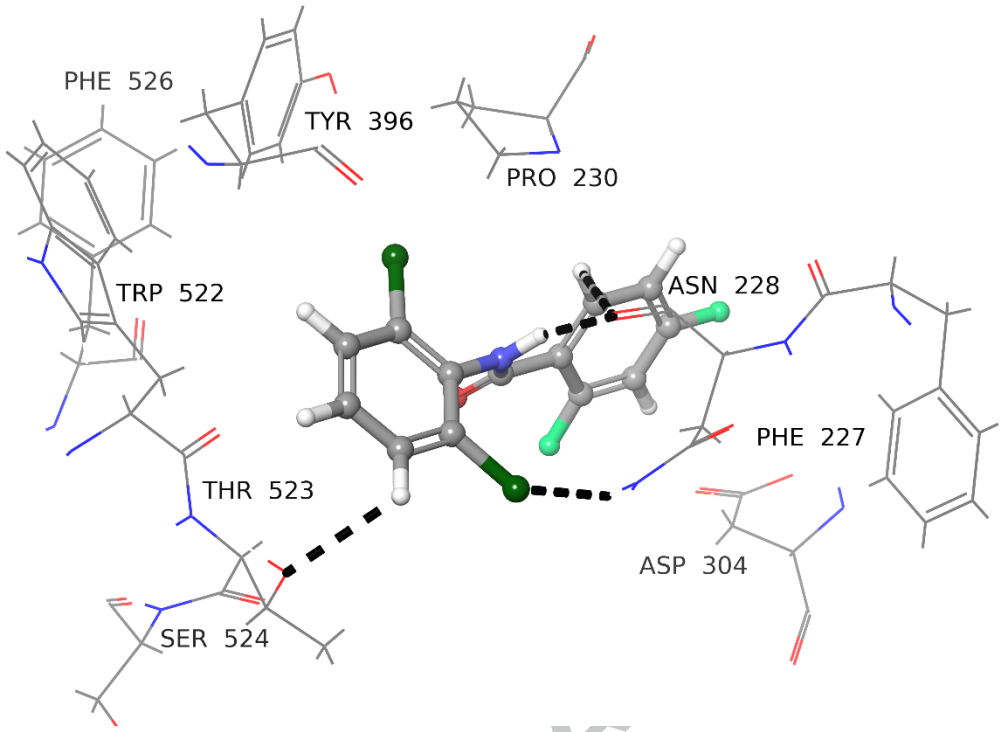

Fig. 13. 3D Representation of docked pose of compound **5** (IC_{50} = 18.7 ± 1.2 μM). Three hydrogen bonds are shown with Asn228 and one with Thr523.

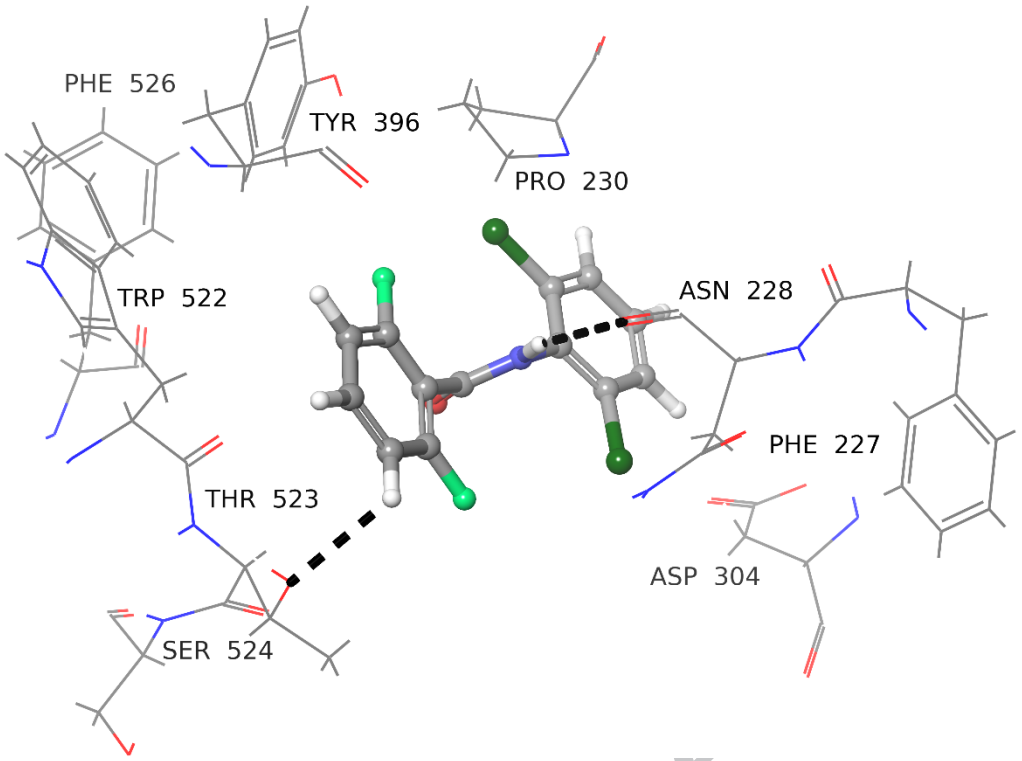

Fig. 14. 3D Representation of docked pose of compound **6** (IC_{50} = 12.6 ± 0.2 μM). Hydrogen bonds are shown with Asn228 and Thr523.

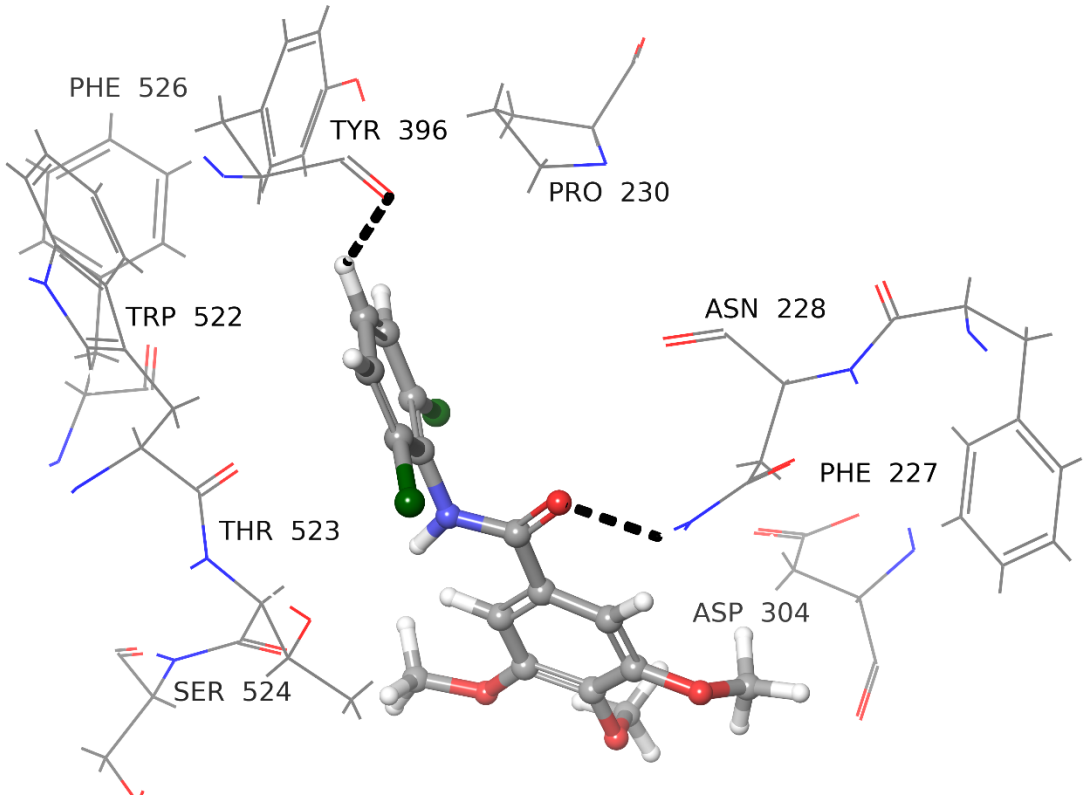

Fig. 15. 3D Representation of docked pose of compound **9** (IC_{50} = 20.8 ± 0.6 μM). Hydrogen bonds are shown with Asn228 and Tyr396.

4. Conclusions

A series of benzamide derivatives **1-12** was designed, synthesized using solvent-free and base-free MAOS methodology and evaluated for their BCHE inhibition. SAR study showed that compounds with halogen substitution had more potent inhibition activity as compared with methoxy, ethoxy and nitro substituted ones. Kinetics and molecular docking studies identified the binding sites of selected inhibitors. The significant inhibitors showed interactions with catalytically important amino acid residues of BCHE such as Glu197, Phe329, Hip438 and many others. Current treatment of Alzheimer`s disease is based on cholinesterase enzyme inhibition (palliative treatment). Although this is not the ultimate cure and other aspect of pathophysiological mechanism need to be considered, but currently anti-cholinesterase's medicines seem to be the only viable option of alleviating the symptoms of AD.

Acknowledgements

Authors are thankful to the Higher Education Commission, Pakistan for providing financial assistance. The authors would like to thank Dr. Rasheeda Swaleh for her constructive criticism in the manuscript.

References

1. Holtzman DM, Morris JC, Goate AM. Alzheimer's disease: the challenge of the second century. Science translational medicine. 2011;3(77):77sr1-sr1.

2. Khan MA, Fazal-ur-Rehman S, Hameed A, Kousar S, Dalvandi K, Yousuf S, Choudhary MI, Basha FZ. Regioselective synthesis of novel 2, 3, 4, 4 a-tetrahydro-1 H-carbazoles and their cholinesterase inhibitory activities. RSC Advances. 2015;5(73):59240-50.

3. Zanetti O, Solerte S, Cantoni F. Life expectancy in Alzheimer's disease (AD). Archives of gerontology and geriatrics. 2009;49:237-43.

4. Aranda-Abreu GE, Hernández-Aguilar ME, Manzo Denes J, García Hernández LI, Herrera Rivero M. Rehabilitating a brain with Alzheimer's: a proposal. Clin Interv Aging. 2011;6:53-9. Epub 02/22. doi: 10.2147/CIA.S14008. PubMed PMID: 21472092.

5. Brookmeyer R, Johnson E, Ziegler-Graham K, Arrighi HM. Forecasting the global burden of Alzheimer's disease. Alzheimer's & dementia. 2007;3(3):186-91.

6. Asojo OA, Ngamelue M, Homma K, Lockridge O. Cocrystallization studies of full-length recombinant butyrylcholinesterase (BChE) with cocaine. Acta Crystallographica Section F: Structural Biology and Crystallization Communications. 2011;67(4):434-7.

7. Darvesh S, Grantham D, Hopkins D. Distribution of butyrylcholinesterase in the human amygdala and hippocampal formation. Journal of Comparative Neurology. 1998;393(3):374-90.

8. Darvesh S, Hopkins DA, Geula C. Neurobiology of butyrylcholinesterase. Nature Reviews Neuroscience. 2003;4(2):131.

9. Liston DR, Nielsen JA, Villalobos A, Chapin D, Jones SB, Hubbard ST, Shalaby IA, Ramirez A, Nason D, White WF. Pharmacology of selective acetylcholinesterase inhibitors: implications for use in Alzheimer's disease. European journal of pharmacology. 2004;486(1):9-17.

10. Xue L, Ko M-C, Tong M, Yang W, Hou S, Fang L, Liu J, Zheng F, Woods JH, Tai H-H. Design, preparation and characterization of high-activity mutants of human butyrylcholinesterase specific for detoxification of cocaine. Molecular pharmacology. 2010:mol. 110.068494.

11. Masson P, Froment M-T, Fortier P-L, Visicchio J-E, Bartels CF, Lockridge O. Butyrylcholinesterase-catalysed hydrolysis of aspirin, a negatively charged ester, and aspirin-related neutral esters. Biochimica et Biophysica Acta (BBA)-Protein Structure and Molecular Enzymology. 1998;1387(1-2):41-52.

12. Mesulam M-M, Guillozet A, Shaw P, Levey A, Duysen E, Lockridge O. Acetylcholinesterase knockouts establish central cholinergic pathways and can use butyrylcholinesterase to hydrolyze acetylcholine. neuroscience. 2002;110(4):627-39.

13. Perry EK, Perry RH, Blessed G, Tomlinson BE. Changes in brain cholinesterases in senile dementia of Alzheimer type. Neuropathology and applied neurobiology. 1978;4(4):273-7. Epub 1978/07/01. PubMed PMID: 703927.

14. Darreh-Shori T, Modiri N, Nordberg A. ApoE and amyloid beta deflate the cholinergic neurotransmission by boosting the activity and stability of cholinesterases in the brain. Alzheimer's & Dementia: The Journal of the Alzheimer's Association. 2009;5(4):P305. doi: 10.1016/j.jalz.2009.04.463.

15. Birks J. Cholinesterase inhibitors for Alzheimer's disease. Cochrane Database Syst Rev. 2006;1(1):CD005593.

16. Gao X-h, Liu L-b, Liu H-r, Tang J-j, Kang L, Wu H, Cui P, Yan J. Structure–activity relationship investigation of benzamide and picolinamide derivatives containing dimethylamine side chain as acetylcholinesterase inhibitors. Journal of enzyme inhibition and medicinal chemistry. 2018;33(1):110-4.

17. Yang X, Peng T, Yang Y, Li W, Xiong J, Zhao L, Ding Z. Antimicrobial and antioxidant activities of a new benzamide from endophytic Streptomyces sp. YIM 67086. Natural product research. 2015;29(4):331-5.

18. Lum RT, Nelson MG, Joly A, Horsma AG, Lee G, Meyer SM, Wick MM, Schow SR. Selective inhibition of the chymotrypsin-like activity of the 20S proteasome by 5-methoxy-1-indanone dipeptide benzamides. Bioorganic & medicinal chemistry letters. 1998;8(3):209-14.

19. Ashton MJ, Cook DC, Fenton G, Karlsson J-A, Palfreyman MN, Raeburn D, Ratcliffe AJ, Souness JE, Thurairatnam S, Vicker N. Selective Type IV Phosphodiesterase Inhibitors as Antiasthmatic Agents. The Syntheses and Biological Activities of 3-(Cyclopentyloxy)-4-methoxybenzamides and Analogs. Journal of Medicinal Chemistry. 1994;37(11):1696-703. doi: 10.1021/jm00037a021.

20. Goto S, Guo Z, Futatsuishi Y, Hori H, Taira Z, Terada H. Quantitative structure-activity relationships of benzamide derivatives for anti-leukotriene activities. Journal of medicinal chemistry. 1992;35(13):2440-5.

21. Tummino PJ, Harvey PJ, McQuade T, Domagala J, Gogliotti R, Sanchez J, Song Y, Hupe D. The human immunodeficiency virus type 1 (HIV-1) nucleocapsid protein zinc ejection activity of disulfide benzamides and benzisothiazolones: correlation with anti-HIV and virucidal activities. Antimicrobial agents and chemotherapy. 1997;41(2):394-400.

22. Kuo J, Hwu H-G. Aripiprazole and haloperidol: beneficial combination antipsychotic therapy for a schizophrenic patient. Clinical neuropharmacology. 2008;31(3):173-5.

23. Chandrasekharan N, Dai H, Roos KLT, Evanson NK, Tomsik J, Elton TS, Simmons DL. COX-3, a cyclooxygenase-1 variant inhibited by acetaminophen and other analgesic/antipyretic drugs: cloning, structure, and expression. Proceedings of the National Academy of Sciences. 2002;99(21):13926-31.

24. Xing Y, Chen S, Zhou Y, Liu N, Chen L, Li Y. Efficient Synthesis of the Nucleus of Atorvastatin Calcium. Synthetic Communications. 2015;45(24):2832-40.

25. Darvesh S, McDonald RS, Penwell A, Conrad S, Darvesh KV, Mataija D, Gomez G, Caines A, Walsh R, Martin E. Structure–activity relationships for inhibition of human cholinesterases by alkyl amide phenothiazine derivatives. Bioorganic & medicinal chemistry. 2005;13(1):211-22.

26. Darvesh S, McDonald RS, Darvesh KV, Mataija D, Conrad S, Gomez G, Walsh R, Martin E. Selective reversible inhibition of human butyrylcholinesterase by aryl amide derivatives of phenothiazine. Bioorganic & medicinal chemistry. 2007;15(19):6367-78.

27. Khan MA, Batool F, Khatoon A, Sadiq R, Rahman S, Basha FZ. Solvent-free protocol for the green synthesis of benzamide analogs of dibenzoazepine. European Journal of Chemistry. 2017;8(2):179-82.

28. Belouezzane C, Pinto AC, Lima AL, Miranda FS. Microwave assisted organic synthesis of benzophenothiazines: Photophysical and DFT calculations studies. Journal of Luminescence. 2017;192:1139-48.

29. Mollo MaC, Orelli LR. Microwave-Assisted Synthesis of 2-Aryl-2-oxazolines, 5, 6-Dihydro-4 H-1, 3-oxazines, and 4, 5, 6, 7-Tetrahydro-1, 3-oxazepines. Organic letters. 2016;18(23):6116-9.

30. Chundawat TS, Sharma N, Kumari P, Bhagat S. Microwave-Assisted Nickel-Catalyzed One-Pot Synthesis of 2, 4, 5-Trisubstituted Imidazoles. Synlett. 2016;27(03):404-8.

31. Laclef S, Harari M, Godeau J, Schmitz-Afonso I, Bischoff L, Hoarau C, Levacher V, Fruit C, Besson T. Ligand-Free Pd-Catalyzed and Copper-Assisted C–H Arylation of Quinazolin-4-ones with Aryl Iodides under Microwave Heating. Organic letters. 2015;17(7):1700-3.

32. Vinson AR, Davis VK, Arunasalam A, Jesse KA, Hamilton RE, Shattuck MA, Hu AC, Iafe RG, Wenzel AG. Gold-Catalyzed, SN1-Type Reaction of Alcohols to Afford Ethers and Cbz-Protected Amines. Synlett. 2015;26(06):765-70.

33. Reilly MK, King RP, Wagner AJ, King SM. Microwave-assisted esterification: a discovery-based microscale laboratory experiment. Journal of Chemical Education. 2014;91(10):1706-9.

34. Yang Q, Wang X-j, Li Z-y, Sun L, You Q-d. Microwave-assisted esterification of diverse carboxylic acids and chiral amino acids. Synthetic Communications®. 2008;38(23):4107-15.

35. Sweygers N, Alewaters N, Dewil R, Appels L. Microwave effects in the dilute acid hydrolysis of cellulose to 5-hydroxymethylfurfural. Scientific reports. 2018;8(1):7719.

36. Schmidt B, Schultze C. A One-Pot Synthesis of Pyranocoumarins Through Microwave-Promoted Propargyl Claisen Rearrangement/Wittig Olefination. European Journal of Organic Chemistry. 2018;2018(2):223-7.

37. Likhar PR, Reddy GN, Reddy MR. Microwave-assisted, water-mediated Michael addition for synthesis of kojic acid derivatives. Research on Chemical Intermediates. 2016;42(6):5983-9.

38. Vanier GS. Microwave-assisted solid-phase peptide synthesis based on the Fmoc protecting group strategy (CEM). Peptide Synthesis and Applications: Springer; 2013. p. 235-49.

39. Kitchen HJ, Vallance SR, Kennedy JL, Tapia-Ruiz N, Carassiti L, Harrison A, Whittaker AG, Drysdale TD, Kingman SW, Gregory DH. Modern microwave methods in solid-state inorganic materials chemistry: from fundamentals to manufacturing. Chemical reviews. 2013;114(2):1170-206.

40. Wang H, Zhu W, Liu Y, Zeng L, Sun L. The Microwave-Assisted Green Synthesis of TiC Powders. Materials. 2016;9(11):904.

41. Dallinger D, Kappe CO. Microwave-assisted synthesis in water as solvent. Chemical Reviews. 2007;107(6):2563-91.

42. Zong L, Zhou S, Sgriccia N, Hawley M, Kempel L. A Review of Microwave-Assist Polymer Chemistry (MAPC). Journal of microwave power and electromagnetic energy. 2003;38(1):49-74.

43. Hasanpoor M, Aliofkhazraei M, Delavari H. Microwave-assisted synthesis of zinc oxide nanoparticles. Procedia Materials Science. 2015;11:320-5.

44. Aivazoglou E, Metaxa E, Hristoforou E. Microwave-assisted synthesis of iron oxide nanoparticles in biocompatible organic environment. AIP Advances. 2018;8(4):048201.

45. Ullah A, Arshad M. Remarkably Efficient Microwave-Assisted Cross-Metathesis of Lipids under Solvent-Free Conditions. ChemSusChem. 2017;10(10):2167-74. Epub 2017/03/02. doi: 10.1002/cssc.201601824. PubMed PMID: 28247590.

46. Arshad M, Pradhan RA, Ullah A. Synthesis of lipid-based amphiphilic block copolymer and its evaluation as nano drug carrier. Mater Sci Eng C Mater Biol Appl. 2017;76:217-23. doi: 10.1016/j.msec.2017.03.109. PubMed PMID: 28482520.

47. Dubois N, Glynn D, McInally T, Rhodes B, Woodward S, Irvine DJ, Dodds C. On DABAL-Me3 promoted formation of amides. Tetrahedron. 2013;69(46):9890-7. doi: https://doi.org/10.1016/j.tet.2013.08.062.

48. Ellman GL, Courtney KD, Andres V, Featherstone RM. A new and rapid colorimetric determination of acetylcholinesterase activity. Biochemical Pharmacology. 1961;7(2):88-95. doi: https://doi.org/10.1016/0006-2952(61)90145-9.

49. Mosmann T. Rapid colorimetric assay for cellular growth and survival: application to proliferation and cytotoxicity assays. J Immunol Methods. 1983;65(1-2):55-63. Epub 1983/12/16. PubMed PMID: 6606682.

50. LigPrep, version 3.6, Schrödinger, LLC, New York, NY, 2015.

51. Glide, version 6.9, Schrödinger, LLC, New York, NY, 2015.

52. Halgren TA. Identifying and characterizing binding sites and assessing druggability. Journal of chemical information and modeling. 2009;49(2):377-89. Epub 2009/05/13. doi: 10.1021/ci800324m. PubMed PMID: 19434839.

53. Schrödinger Release 2015-4: SiteMap, version 3.7, Schrödinger, LLC, New York, NY, 2015.

54. Bajda M, Więckowska A, Hebda M, Guzior N, Sotriffer CA, Malawska B. Structure-based search for new inhibitors of cholinesterases. Int J Mol Sci. 2013;14(3):5608-32. doi: 10.3390/ijms14035608. PubMed PMID: 23478436.

Highlights

- Microwave-Assisted Organic Synthesis is a facile method for the synthesis of benzamide derivatives.
- Benzamides of 2,6-dichloroaniline showed selective *in vitro* butyrylcholinesterase (BCHE) inhibitory activity.
- 4-Bromosubstituted benzamide of 2,6-dichloroaniline (IC_{50} value = 0.8 ± 0.6 μM) was the most active analogue.
- Enzyme kinetic studies of synthesized compounds showed mixed as well as uncompetitive types of inhibition.

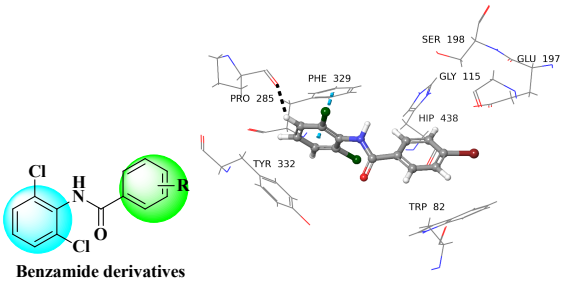

Benzamide derivatives